



HBx interacts with Bcl-2 and Bcl-xL in human hepatic HepG2 cells by coimmunoprecipitation assay. In HepG2 cells transfected with pcDNA3.1-Flag-HBx, endogenous Bcl-2 and Bcl-xL, but not the anti-apoptotic Bcl-2 family member Mcl-1, were coprecipitated with Flag-HBx, using an antibody to the Flag epitope (Fig. 1A, lane 3). In contrast, no Bcl-xL and only a trace amount of Bcl-2 were coprecipitated with Flag-HBx(G124L, I127A) (Fig. 1A, lane 4), which was expressed in HepG2 cells at a comparable level to Flag-HBx (Fig. 1A, lanes 1 and 2). These results indicate that HBx associates with Bcl-2 and Bcl-xL in human cells through its BH3-like motif. Importantly, in HepG2 cells transfected with a 140% head-to-tail DNA copy of the HBV genome (pHBV) with or without HBx(G124L, I127A) mutations, endogenous Bcl-2 and Bcl-xL, but not Mcl-1, were coprecipitated with HBx, but not with HBx(G124L, I127A), using an antibody to HBx (Fig. 1B, lanes 3 and 4). Therefore, HBx expressed from its native promoter in a replicating HBV genome associates with endogenous Bcl-2 and Bcl-xL in human hepatic cells through its BH3-like motif.

**HBx Induces Cell Killing and Cytosolic Calcium Increase in Hepatocytes Through Its BH3-Like Motif.** We analyzed the cell-killing activity of HBx in human cells by staining HBx-transfected HepG2 cells with Annexin-V Pacific Blue and propidium iodide (PI) to distinguish living cells from apoptotic and necrotic cells. Flow cytometry analysis of cells transfected with pcDNA3.1-Flag-HBx showed 10.6% apoptotic cells (Annexin-V positive and PI negative) and 7.9% necrotic cells (Annexin-V positive and PI positive) (Fig. 2B). Significantly less cell death was observed in HepG2 cells transfected with the same amount of pcDNA3.1-Flag-HBx(G124L, I127A) (4.87% apoptotic cells and 1.14% necrotic cells; Fig. 2C) or empty pcDNA3.1 vector (1.14% apoptotic cells and 0.32% necrotic cells; Fig. 2A). Therefore, as in *C. elegans*, HBx uses its BH3-like motif to bind anti-apoptotic Bcl-2 and Bcl-xL proteins and induces both apoptosis and necrosis in human hepatocytes.

Because calcium signaling is an important event downstream of HBx, we examined whether the BH3-like motif of HBx is

necessary for HBx-induced elevation of cytosolic calcium. Cytosolic calcium in HepG2 cells transfected with pcDNA3.1-Flag-HBx or pcDNA3.1-Flag-HBx(G124L, I127A) was determined using the ratiometric fluorescent calcium indicator Fura-2 (27). We found that the resting calcium concentration was significantly increased upon expression of HBx compared with the vector-only control (Fig. 1C), whereas expression of HBx(G124L, I127A) failed to do so. The HBx-induced calcium elevation is not due to increased cell death, because a similar level of calcium increase was observed in the presence of Z-VAD, a pan-caspase inhibitor that blocks cell death (Fig. S1A). These results indicate that HBx can induce an increase in cytosolic calcium that is dependent on its BH3-like motif and association with Bcl-2 family proteins.

**BH3-Like Motif of HBx Is Critical for HBV Viral Replication.** Given the critical role of HBx in HBV DNA replication (20), we examined whether interactions between HBx and Bcl-2 proteins are important for HBV replication. Cytoplasmic viral core particles, where HBV DNA replication occurs, were isolated from HepG2 cells transfected with the pHBV replicon with or without the HBx(G124L, I127A) mutations. The level of HBV DNA replication was examined by Southern blot analysis. Compared with cells transfected with wild-type pHBV, HBV DNA replication was significantly reduced in cells transfected with the mutant pHBV (Fig. 3A). The level of the HBV core protein (HBcAg), which correlates with the level of HBV DNA (28), was also greatly reduced in cells transfected with the mutant HBV genome (Fig. 3B). Northern blot analysis showed no reduction in HBV pregenomic (pg)/precore (pc) RNA, preS/S mRNA, or HBx mRNA in cells transfected with the mutant pHBV replicon (Fig. 3C). Quantitative real-time PCR (Q-PCR) analysis of isolated viral particles revealed an eight- to ninefold reduction in HBV DNA replication in cells transfected with the mutant HBV genome compared with cells transfected with the wild-type HBV genome (Fig. 3D). These results indicate that the BH3-like motif of HBx is critical for HBV DNA replication but dispensable for HBV transcription. Importantly, HBV DNA replication in cells

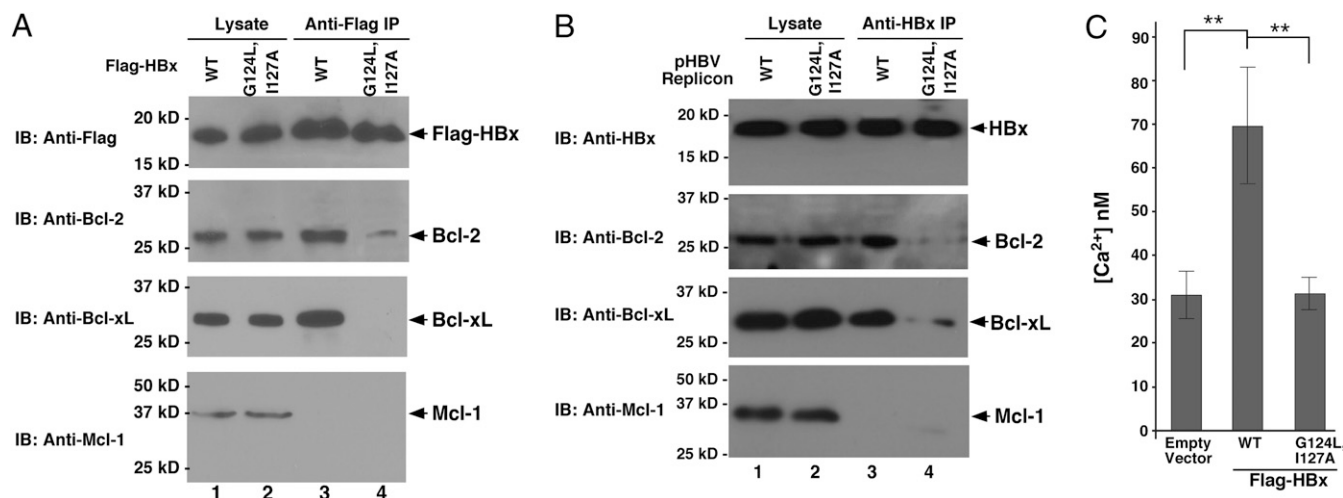
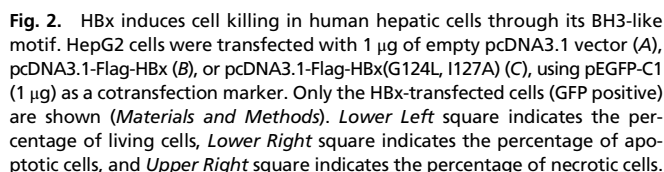


**Fig. 1.** HBx binds Bcl-2 and Bcl-xL and induces elevation of cytosolic  $Ca^{2+}$  in human hepatocytes through its BH3-like motif. (A) HBx associates with Bcl-2 and Bcl-xL in HepG2 cells. A coimmunoprecipitation (co-IP) experiment was performed in HepG2 cells transfected with pcDNA3.1-Flag-HBx or pcDNA3.1-Flag-HBx(G124L, I127A) (Materials and Methods). The cell lysate was precipitated with an anti-Flag antibody and analyzed by immunoblotting (IB), using anti-Flag, anti-Bcl-2, anti-Bcl-xL, and anti-Mcl-1 antibodies, respectively (lanes 3 and 4). One portion of the cell lysate was used in immunoblotting analysis to examine the expression levels of the HBx protein and Bcl-2 family proteins (lanes 1 and 2). (B) HBx expressed from its native promoter in a replicating HBV genome binds Bcl-2 and Bcl-xL in HepG2 cells. The co-IP experiment was performed as in A. The cell lysate was precipitated with an anti-HBx monoclonal antibody (16F9) and analyzed by IB analysis as in A. (C) Expression of HBx in HepG2 cells increases cytosolic  $Ca^{2+}$  through the BH3-like motif. HepG2 cells cotransfected with pcDNA3-mCherry and pcDNA3.1-Flag-HBx or pcDNA3.1-Flag-HBx(G124L, I127A) were treated with 4  $\mu$ M Fura-2-AM 48 h posttransfection.  $Ca^{2+}$  concentrations were calculated from the measured Fura-2 ratios as previously described (27). Error bars indicate SEM ( $n > 12$ ).  $^{**}P < 0.01$ .



We next examined the importance of HBx interaction with Bcl-2 proteins for HBV replication in an established mouse model of chronic HBV infection (30). The pHBV replicon with wild-type HBx or HBx(G124L, I127A) was introduced into

**Bcl-2 and Bcl-xL Are Important for HBx-Induced Cytosolic Calcium Elevation and HBV Viral Replication in Hepatocytes.** We examined the importance of Bcl-2 proteins for HBV replication by knocking down the expression of Bcl-2 or Bcl-xL in HepG2 cells through RNA interference (RNAi). Compared with control short hairpin RNA (shRNA), Bcl-2 and Bcl-xL shRNA significantly reduced the expression of Bcl-2 and Bcl-xL in HepG2 cells, respectively (Fig. 5 *A* and *B*). Importantly, Q-PCR analysis of isolated viral particles revealed a 21–41% reduction in HBV DNA replication in cells infected by lentivirus expressing Bcl-2 or Bcl-xL shRNA, compared with cells with control shRNA (Fig. 5 *A* and *B*). Overexpression of the anti-apoptotic Mcl-1 protein, which does not interact with HBx (Fig. 1 *A* and *B*), in cells treated with Bcl-2 or Bcl-xL shRNA did not prevent reduction of HBV DNA replication (Fig. S2), indicating that decreased HBV DNA replication caused by loss of Bcl-2 or Bcl-xL is unlikely due to impaired survival of the host cells. Moreover, RNAi knockdown of Bcl-2 or Bcl-xL dampened but did not obliterate intracellular calcium increase induced by HBx (Fig. S1 *B* and *C*), which is consistent with the finding that Bcl-2 or Bcl-xL knockdown reduced but did not block HBV DNA replication and indicates that Bcl-2 and Bcl-xL are partially redundant in mediating HBx functions. Bcl-2 and Bcl-xL double-knockdown cells were not viable for analysis of HBV viral replication and intracellular calcium changes. These results indicate that Bcl-2 and Bcl-xL are important for HBV viral replication and, together with the findings described above, provide strong evidence that HBx targets both Bcl-2 and Bcl-xL to increase intracellular calcium and to promote HBV DNA replication (Fig. 5*C*).

Despite the critical role of HBx in HBV pathogenesis and oncogenesis, identification of HBx host targets has remained a major challenge in the last three decades (1, 2, 7). The intricacy of HBx activities, the lack of a powerful animal model to study HBV infection, variability among cell culture assays, and the complexity of the mammalian genome, which encodes at least six Bcl-2 family proteins, have all contributed to the longstanding questions regarding the functions of HBx, its interactions with host targets, and its mechanisms of action. We have engineered a *C. elegans* animal model to identify HBx targets and downstream signaling pathways (26). Mimicking the initial cellular events that unfold following liver infection by HBV (17, 31, 32), HBx induces both apoptosis and necrosis in *C. elegans* through canonical cell death pathways. Interestingly, a unique gain-of-function mutation (G169E) in the Bcl-2 homolog CED-9, which inhibits cell death in *C. elegans* by blocking the binding of the endogenous BH3-only cell death inducer EGL-1 to CED-9 (33), also completely blocks the interaction between CED-9 and the BH3-like motif of HBx and HBx-induced cell death in *C. elegans*. Remarkably, Bcl-2 can fully substitute for CED-9 in *C. elegans* to mediate HBx-induced cell killing, indicating that Bcl-2 likely interacts with HBx in mammals. Indeed, we demonstrate here that HBx associates with Bcl-2 and Bcl-xL in human hepatocytes.



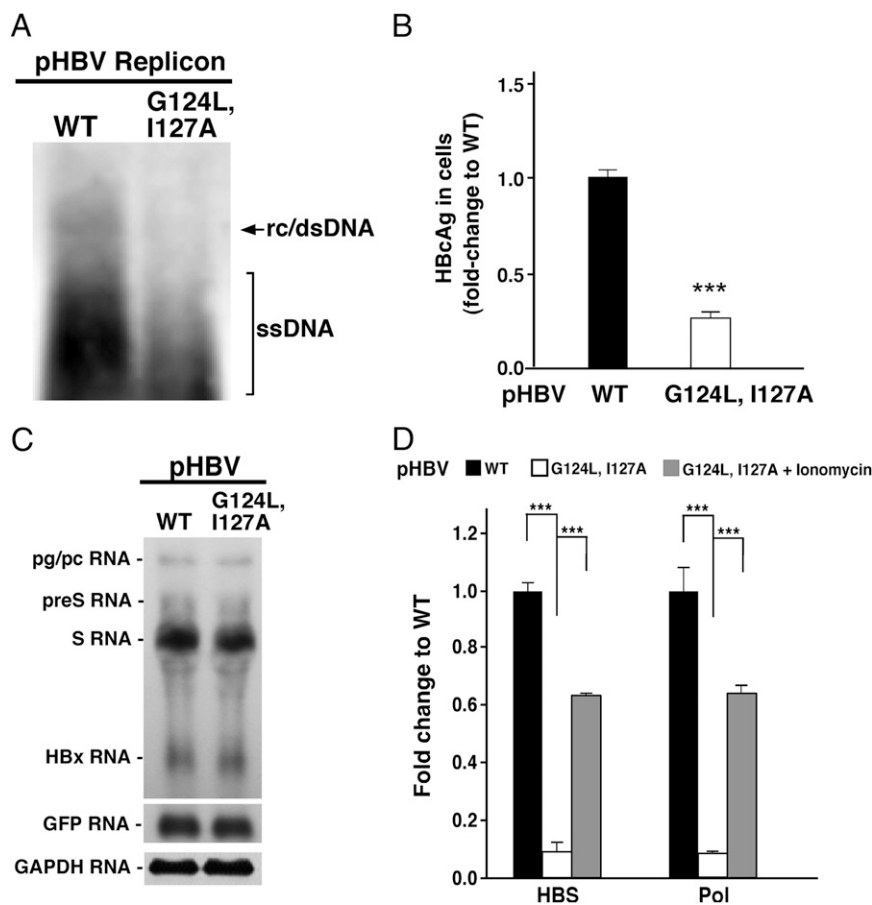


**Fig. 3.** Interaction between HBx and Bcl-2 proteins is critical for HBV DNA replication in human hepatic cells. (A) Southern blot analysis of HBV DNA replication in HepG2 cells transfected with the wild-type or mutant (G124L, I127A) pHBV replicon 3 d posttransfection. rc/ds DNA represents relaxed circular DNA and double-stranded DNA. ssDNA represents single-stranded DNA. (B) Measurement of the levels of the HBV core protein (HbcAg) in transfected HepG2 cells. The difference between cells transfected with the wild-type and mutant (G124L, I127A) pHBV is shown as fold change to wild type. The data represent mean  $\pm$  SD from three independent experiments. \*\*\* $P < 0.0001$ . (C) Northern blot analysis of HBV transcription in HepG2 cells transfected with the wild-type or mutant pHBV replicon 3 d posttransfection. Different pHBV mRNAs are indicated. GFP mRNA from a cotransfection marker and Glyceraldehyde-3-phosphate dehydrogenase (GAPDH) mRNA were used as controls. (D) Quantitative PCR analysis of HBV DNA replication in HepG2 cells transfected with the wild-type or mutant pHBV replicon with or without 5  $\mu$ M ionomycin treatment. Three days posttransfection, cytoplasmic HBV viral particles were isolated and the viral DNA replication intermediates were quantified by real-time PCR (Materials and Methods). The results represent the fold change of the replicative intermediates from the mutant pHBV replicon compared with those from the wild-type pHBV replicon in HepG2 cells, using two different primer sets (one specific to the HBS ORF and one specific to the polymerase ORF). Data are presented as mean  $\pm$  SEM. At least three independent experiments were performed for each dataset. \*\*\* $P < 0.0001$ .

through its BH3-like motif and that this protein interaction is crucial for HBx-induced cytosolic calcium elevation, cell death, and viral DNA replication. These findings suggest that molecular mimicry of endogenous BH3-only proteins by HBx enables its interactions with conserved host targets and hijacking of cell signaling pathways to benefit viral infection.

Calcium signaling is a critical event downstream of HBx expression that promotes HBV replication, core assembly, cell death, and other HBx functions (2, 20, 21, 25). HBx has been proposed to effect MPT (4–6, 20), which is important for intracellular calcium homeostasis and cell death (34, 35).

Importantly, both Bcl-2 and Bcl-xL are mitochondrial proteins and have been implicated in regulating MPT (34, 36). HBx binding to Bcl-2 and Bcl-xL is critical for calcium regulation by HBx, because expression of HBx, but not HBx(G124L, I127A), which fails to bind Bcl-2 and Bcl-xL, triggers elevation of cytosolic calcium in hepatocytes. The finding that G124L/I127A mutations in the BH3-like motif of HBx greatly reduce HBV DNA replication in human and mouse hepatocytes, which can be substantially rescued by restoring cytosolic calcium with ionomycin, and the observation that RNAi knockdown of either Bcl-2 or Bcl-xL significantly compromises HBx-induced intracellular

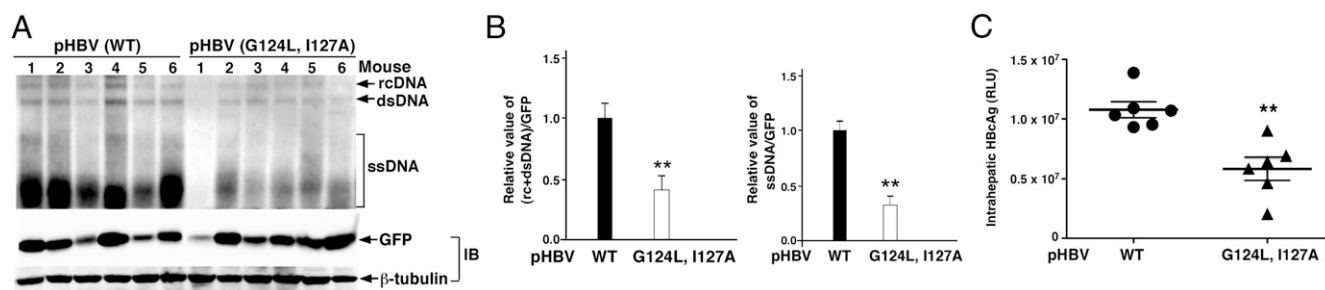


**Fig. 4.** Interaction between HBx and Bcl-2 proteins is critical for HBV DNA replication in mouse hepatocytes. (A) Southern blot analysis of HBV DNA replication in mouse livers after hydrodynamical injection of the wild-type or the mutant (G124L, I127A) pHBV replicon 2 d postinjection. pcDNA3-GFP was coinjected as an injection marker. Equivalent amounts of liver tissues from six BALB/C mice in each injection group were collected and subjected to HBV DNA and HbcAg analyses (Materials and Methods). The levels of GFP and  $\beta$ -tubulin were determined by immunoblotting (IB) and used as controls to normalize the transfection efficiency. (B) Quantification of viral DNA intermediates from the Southern blot analysis in A. The results represent the relative value of different HBV DNA intermediates to the GFP control. The amounts of DNA and GFP were quantified by Quantity One software (Bio-Rad). Data are presented as mean  $\pm$  SEM. \*\* $P < 0.01$ . (C) A plot showing the levels of the HBV core protein (HbcAg) in mouse livers. All mice ( $n = 6$ ) from each injection group were subjected to HbcAg analysis (Materials and Methods). RLU represents relative luminescence units (mean  $\pm$  SEM). \*\* $P < 0.01$ .

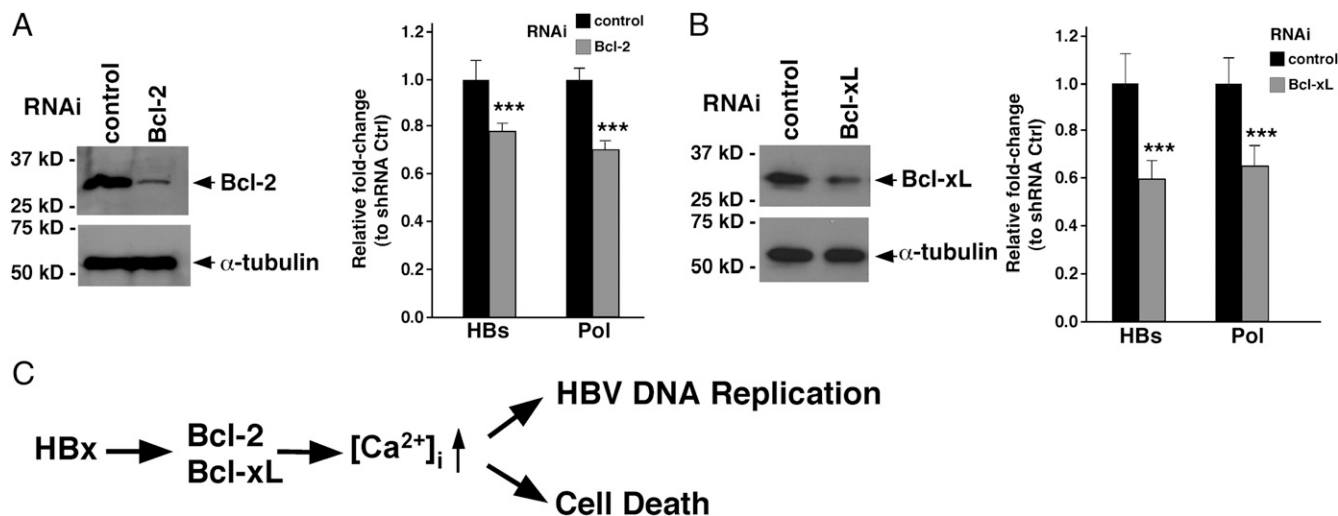


**Fig. 5.** Bcl-2 and Bcl-xL are important for HBV DNA replication. (A and B) (Right) HepG2 cells infected by lentivirus expressing control, Bcl-2, or Bcl-xL shRNA were transfected with the pHBV replicon and subjected to Q-PCR analysis as described in Fig. 3D. (Left) One portion of the cells was analyzed by immunoblotting to examine the expression levels of Bcl-2 and Bcl-xL, using  $\alpha$ -tubulin as a loading control. Data are presented as mean  $\pm$  SEM. \*\*\* $P < 0.0001$ . (C) A working model of HBx-dependent viral pathogenesis. HBx directly interacts with Bcl-2 and Bcl-xL to increase cytosolic  $\text{Ca}^{2+}$ . Increased cytosolic  $\text{Ca}^{2+}$  then promotes HBV replication and cell death. This signaling pathway is conserved in *C. elegans*.

calcium increase and HBV replication provide further confirmation that HBx targets Bcl-2 proteins to trigger cytosolic calcium elevation required for HBV replication and other events such as cell death (Fig. 5C).

Hepatocarcinogenesis is a complex and poorly understood process. Chronic hepatocyte cell death induced by HBV infection or carcinogens may trigger cycles of inflammation, immune response, and compensatory tissue regeneration and the acquisition of oncogenic mutations that lead to development of HCC (17, 31, 37). On the other hand, hepatocyte expression of prosurvival factors, such as Bcl-2 and p38 $\alpha$  kinase, has been shown to be effective in preventing HCC development (37–39). Moreover, HBV viral replication plays an important contributing role in hepatocarcinogenesis. The development and progression of HCC in patients with chronic HBV strongly correlate with the viral DNA level in a dose-dependent manner (40, 41). Therefore, blocking HBV viral replication and HBV-induced cell death represents an effective strategy to treat patients with chronic HBV and to prevent the development of HCC. Our study suggests that the BH3-like motif of HBx is necessary for HBx binding to Bcl-2 family proteins, which results in elevated cytosolic calcium, efficient viral replication, and HBV-induced cell death. Therefore, therapeutically targeting the BH3-like motif of HBx could be a unique and effective strategy to treat patients with chronic HBV and to prevent development of HCC.

## Materials and Methods

**Immunoprecipitation Assays.** HepG2 cells transfected with the pcDNA3.1-Flag-HBx constructs or the pHBV replicons (wild-type and G124L/127A mutations) were lysed and precipitated using an anti-Flag antibody or an anti-HBx

antibody. The proteins pulled down with HBx were detected by immunoblotting analysis.

**Calcium Imaging and Analysis.** HepG2 cells cotransfected with pcDNA3-mCherry and pcDNA3.1-Flag-HBx constructs (wild-type or G124L/127A mutations) were incubated for 35 min with 4  $\mu\text{M}$  Fura-2-AM and 0.04% Pluronic solution 48 h posttransfection, washed three times with buffer, and incubated for an additional 15 min to allow for cleavage of the acetoxymethyl (AM) ester, which trapped Fura-2 in the cells. Data were collected using the Metafluor software and analyzed by Excel (27). Statistical analysis was performed using a *t* test in the Kaleidagraph program. The error bars indicate SEM.

**Quantification of HBV DNA Replication and HBcAg.** Southern hybridization analysis and quantitative real-time PCR were used to quantify the amount of HBV replication DNA intermediates isolated from HepG2 cells or from mouse livers. The level of cytoplasmic HBcAg was measured by chemiluminescence, using a commercial assay kit.

**Hydrodynamic Injection.** Thirty micrograms of the pHBV replicon and 3  $\mu\text{g}$  of pcDNA3-GFP were injected into the tail veins of BALB/c mice within 5 s in a volume of PBS equivalent to 10% of the mouse body weight. Livers of the injected mice were assayed for HBcAg and viral DNA 2 d after injection (30).

Detailed methods are available in *SI Materials and Methods*.

**ACKNOWLEDGMENTS.** We thank T. Blumenthal and R. Garcea for comments and suggestions. This work was supported by National Institutes of Health Grants F30 NS070596 (to B.L.H.); R01 GM059083, GM079097, and GM088241 (to D.X.); and GM084027 (to A.E.P.); grants from China National Science Foundation (30925030) and the National Scientific and Technological Major Project (2013ZX10002-002) (to N.-S.X.); and a Burroughs Wellcome Fund Award (to D.X.).

- Kremsdorff D, Soussan P, Paterlini-Brechot P, Brechot C (2006) Hepatitis B virus-related hepatocellular carcinoma: Paradigms for viral-related human carcinogenesis. *Oncogene* 25:3823–3833.
- Ganem D, Schneider RJ (2001) The molecular biology of the hepatitis B viruses. *Fields Virology*, eds Knipe DM, et al. (Lippincott Williams & Wilkins, Philadelphia), 4th Ed, Vol 2, pp 2923–2970.
- Terradillos O, et al. (2002) The hepatitis B virus X protein abrogates Bcl-2-mediated protection against Fas apoptosis in the liver. *Oncogene* 21:377–386.
- Shirakata Y, Koike K (2003) Hepatitis B virus X protein induces cell death by causing loss of mitochondrial membrane potential. *J Biol Chem* 278:22071–22078.
- Clippinger AJ, Gearhart TL, Bouchard MJ (2009) Hepatitis B virus X protein modulates apoptosis in primary rat hepatocytes by regulating both NF- $\kappa$ B and the mitochondrial permeability transition pore. *J Virol* 83:4718–4731.

- Rahmani Z, Huh KW, Lasher R, Siddiqui A (2000) Hepatitis B virus X protein colocalizes to mitochondria with a human voltage-dependent anion channel, HVDAC3, and alters its transmembrane potential. *J Virol* 74:2840–2846.
- Wei Y, Neuveut C, Tiollais P, Buendia MA (2010) Molecular biology of the hepatitis B virus and role of the X gene. *Pathol Biol (Paris)* 58:267–272.
- Feitelson MA, Duan LX (1997) Hepatitis B virus X antigen in the pathogenesis of chronic infections and the development of hepatocellular carcinoma. *Am J Pathol* 150:1141–1157.
- Su Q, et al. (1998) Expression of hepatitis B virus X protein in HBV-infected human livers and hepatocellular carcinomas. *Hepatology* 27:1109–1120.
- Peng Z, et al. (2005) Integration of the hepatitis B virus X fragment in hepatocellular carcinoma and its effects on the expression of multiple molecules: A key to the cell cycle and apoptosis. *Int J Oncol* 26:467–473.

11. Sirma H, et al. (1999) Hepatitis B virus X mutants, present in hepatocellular carcinoma tissue abrogate both the antiproliferative and transactivation effects of HBx. *Oncogene* 18:4848–4859.
12. Tu H, et al. (2001) Biological impact of natural COOH-terminal deletions of hepatitis B virus X protein in hepatocellular carcinoma tissues. *Cancer Res* 61:7803–7810.
13. Kim CM, Koike K, Saito I, Miyamura T, Jay G (1991) HBx gene of hepatitis B virus induces liver cancer in transgenic mice. *Nature* 351:317–320.
14. Terradillos O, et al. (1997) The hepatitis B virus X gene potentiates c-myc-induced liver oncogenesis in transgenic mice. *Oncogene* 14:395–404.
15. Yu DY, et al. (1999) Incidence of hepatocellular carcinoma in transgenic mice expressing the hepatitis B virus X-protein. *J Hepatol* 31:123–132.
16. Madden CR, Finegold MJ, Slagle BL (2001) Hepatitis B virus X protein acts as a tumor promoter in development of diethylnitrosamine-induced preneoplastic lesions. *J Virol* 75:3851–3858.
17. Wu BK, et al. (2006) Blocking of G1/S transition and cell death in the regenerating liver of Hepatitis B virus X protein transgenic mice. *Biochem Biophys Res Commun* 340:916–928.
18. Bouchard MJ, Schneider RJ (2004) The enigmatic X gene of hepatitis B virus. *J Virol* 78:12725–12734.
19. Choi Y, Gyoo Park S, Yoo JH, Jung G (2005) Calcium ions affect the hepatitis B virus core assembly. *Virology* 332:454–463.
20. Bouchard MJ, Wang LH, Schneider RJ (2001) Calcium signaling by HBx protein in hepatitis B virus DNA replication. *Science* 294:2376–2378.
21. Bouchard MJ, Puro RJ, Wang L, Schneider RJ (2003) Activation and inhibition of cellular calcium and tyrosine kinase signaling pathways identify targets of the HBx protein involved in hepatitis B virus replication. *J Virol* 77:7713–7719.
22. Tarn C, Zou L, Hullinger RL, Andrisani OM (2002) Hepatitis B virus X protein activates the p38 mitogen-activated protein kinase pathway in dedifferentiated hepatocytes. *J Virol* 76:9763–9772.
23. Oh JC, Jeong DL, Kim IK, Oh SH (2003) Activation of calcium signaling by hepatitis B virus-X protein in liver cells. *Exp Mol Med* 35:301–309.
24. Lara-Pezzi E, Armesilla AL, Majano PL, Redondo JM, López-Cabrera M (1998) The hepatitis B virus X protein activates nuclear factor of activated T cells (NF-AT) by a cyclosporin A-sensitive pathway. *EMBO J* 17:7066–7077.
25. Chami M, Ferrari D, Nicotera P, Paterlini-Bréchet P, Rizzuto R (2003) Caspase-dependent alterations of Ca<sup>2+</sup> signaling in the induction of apoptosis by hepatitis B virus X protein. *J Biol Chem* 278:31745–31755.
26. Geng X, et al. (2012) *Proc Natl Acad Sci USA*, 10.1073/pnas.1204652109.
27. Gryniewicz G, Poenie M, Tsien RY (1985) A new generation of Ca<sup>2+</sup> indicators with greatly improved fluorescence properties. *J Biol Chem* 260:3440–3450.
28. Kimura T, et al. (2003) New enzyme immunoassay for detection of hepatitis B virus core antigen (HBcAg) and relation between levels of HBcAg and HBV DNA. *J Clin Microbiol* 41:1901–1906.
29. Morgan AJ, Jacob R (1994) Ionomycin enhances Ca<sup>2+</sup> influx by stimulating store-regulated cation entry and not by a direct action at the plasma membrane. *Biochem J* 300:665–672.
30. Huang LR, Wu HL, Chen PJ, Chen DS (2006) An immunocompetent mouse model for the tolerance of human chronic hepatitis B virus infection. *Proc Natl Acad Sci USA* 103:17862–17867.
31. Pollicino T, Terradillos O, Lecoer H, Gougeon ML, Buendia MA (1998) Pro-apoptotic effect of the hepatitis B virus X gene. *Biomed Pharmacother* 52:363–368.
32. Guo JT, et al. (2000) Apoptosis and regeneration of hepatocytes during recovery from transient hepatitis B virus infections. *J Virol* 74:1495–1505.
33. Parrish J, Metters H, Chen L, Xue D (2000) Demonstration of the in vivo interaction of key cell death regulators by structure-based design of second-site suppressors. *Proc Natl Acad Sci USA* 97:11916–11921.
34. Zhivotovsky B, Galluzzi L, Kepp O, Kroemer G (2009) Adenine nucleotide translocase: A component of the phylogenetically conserved cell death machinery. *Cell Death Differ* 16:1419–1425.
35. Bernardi P, Rasola A (2007) Calcium and cell death: The mitochondrial connection. *Subcell Biochem* 45:481–506.
36. Breckenridge DG, Xue D (2004) Regulation of mitochondrial membrane permeabilization by BCL-2 family proteins and caspases. *Curr Opin Cell Biol* 16:647–652.
37. Sakurai T, et al. (2008) Hepatocyte necrosis induced by oxidative stress and IL-1 alpha release mediate carcinogen-induced compensatory proliferation and liver tumorigenesis. *Cancer Cell* 14:156–165.
38. Pierce RH, Vail ME, Ralph L, Campbell JS, Fausto N (2002) Bcl-2 expression inhibits liver carcinogenesis and delays the development of proliferating foci. *Am J Pathol* 160:1555–1560.
39. Maeda S, Kamata H, Luo JL, Leffert H, Karin M (2005) IKKbeta couples hepatocyte death to cytokine-driven compensatory proliferation that promotes chemical hepatocarcinogenesis. *Cell* 121:977–990.
40. Chen CJ, et al.; REVEAL-HBV Study Group (2006) Risk of hepatocellular carcinoma across a biological gradient of serum hepatitis B virus DNA level. *JAMA* 295:65–73.
41. Yuen MF, et al. (2008) Risk for hepatocellular carcinoma with respect to hepatitis B virus genotypes B/C, specific mutations of enhancer II/core promoter/precore regions and HBV DNA levels. *Gut* 57:98–102.

# Supporting Information

Geng et al. 10.1073/pnas.1204668109

## SI Materials and Methods

**Molecular Biology.** The hepatitis B virus (HBV) X protein (HBx) cDNA clone was kindly provided by Xiao-Kun Zhang (Burnham Institute for Medical Research, La Jolla, CA). Standard methods of cloning, sequencing, and PCR amplification were used. To make HBx mammalian expression constructs, a DNA fragment encoding Flag-HBx was amplified by PCR and subcloned into the pcDNA3.1(+) vector via its NheI and EcoRV sites. The HBx mutant constructs containing G124L and I127A substitutions were generated using a QuikChange Site-Directed Mutagenesis kit (Stratagene) and confirmed by DNA sequencing. The pHBV replicon contains a 140% DNA copy of the HBV genome and replicates in an HBx-dependent manner in HepG2 cells. pHBV containing HBx(G124L, I127A) was made by Quick-Change site-directed mutagenesis and confirmed by DNA sequencing.

**Cell Culture.** Human HepG2 cells were grown in DMEM with 10% (vol/vol) FBS (Sigma-Aldrich). Transfection of HepG2 cells was carried out using Effectene Transfection Reagent (Qiagen), following the manufacturer's protocol. A transfection efficiency of 15–30% was routinely achieved. All transfection experiments were performed 24 h after plating. One microgram of pcDNA3.1, pcDNA3.1-Flag-HBx, or pcDNA3.1-Flag-HBx(G124L, I127A) was diluted in 100  $\mu$ L of the DNA-condensation buffer (Buffer EC) supplied by the manufacturer (Qiagen). Eight microliters of enhancer and 10  $\mu$ L of Effectene were sequentially added to the mixture, each followed by vortexing and incubation at room temperature per manufacturer's protocol. After that, the mixture was supplemented with 0.6 mL complete medium and added to cells. Cotransfection of an enhanced GFP (EGFP)-expressing plasmid pEGFP-C1 (1  $\mu$ g) was included, where appropriate, to monitor transfection efficiency when performing flow cytometry analysis in the cell-killing assays.

**Coimmunoprecipitation Assays.** Coimmunoprecipitation experiments were performed using an antibody (M2) to the Flag epitope (Sigma) or an anti-HBx antibody (16F9). Briefly, HepG2 cells transfected with pcDNA3.1-Flag-HBx or pHBV constructs (wild type or mutant) were lysed in lysis buffer [100 mM NaCl, 0.5 mM  $MgCl_2$ , 0.15 mM  $CaCl_2$ , 1% (vol/vol) Nonidet P-40, 10 mM Tris-HCl, pH 8.0] containing protease inhibitor mixture tablets (Roche). Cell debris was removed by centrifugation at  $10,000 \times g$  for 10 min at 4 °C. The cell lysate was precleared with Protein G Sepharose beads (GE Healthcare) and subsequently incubated with the M2 or 16F9 antibody for 1 h with gentle shaking at 4 °C. Protein G Sepharose beads were then added and the incubation continued for another 2 h. The beads were washed five times with the lysis buffer. The bound proteins were resolved on a 15% SDS polyacrylamide gel and detected by immunoblotting, using anti-Bcl-2, anti-Bcl-xL, and anti-Mcl-1 antibodies (Cell Signaling Technology), respectively.

**Flow Cytometry.** Thirty-six hours posttransfection, living and dead HepG2 cells were scraped into the cell growth medium and precipitated by centrifugation. Cells from one well of a six-well plate ( $\sim 6 \times 10^5$  cells) were washed in cold PBS twice and resuspended in 600  $\mu$ L Annexin V-binding buffer (10 mM Hepes, 140 mM NaCl, and 2.5 mM  $CaCl_2$ , pH 7.4). Labeling of cells by propidium iodide (Sigma) and Annexin-V Pacific Blue (Invitrogen) was carried out according to the protocol provided by Invitrogen. Briefly, 100  $\mu$ L of the suspended cells were transferred to a new tube. Five microliters of Annexin-V Pacific Blue (Invitrogen) and

5  $\mu$ L of propidium iodide (Sigma) were added to each tube and incubated for 30 min at room temperature in the dark. Four hundred microliters of Annexin-V binding buffer were then added to each tube. Cells were analyzed on the CyAn ADP Analyzer (DakoCytomation) with background gates set to exclude non-transfected GFP(–) cells and to restrict Annexin-V Pacific Blue staining alone, or propidium iodide staining alone, to fewer than 0.5% positive events. Data were collected from more than 10,000 cells for each sample.

**Cytosolic Calcium Measurement.** HepG2 cells were cotransfected with pcDNA3-mcherry and pcDNA3.1-Flag-HBx constructs (wild type or mutant), using lipofectamine LTX (Invitrogen). After 48 h or later, cells were washed with HBBSS buffer (Hank's Balanced Salt Solution supplemented with 20 mM Hepes and 11 mM glucose) three times and then incubated with 4  $\mu$ M Fura-2-AM and 0.04% Pluronic solution for 35 min. Cells were rinsed with HBBSS three times and left with HBBSS for another 15 min to allow for cleavage of the acetoxymethyl (AM) ester, trapping Fura-2 inside the cells.

Imaging experiments were performed on an Axiovert 200M inverted fluorescence microscope (Zeiss) with a Cascade 512B CCD camera (Roper Scientific), equipped with a Xenon Arc lamp (XBO75), 340/26 and 380/10 excitation filters, a 450-nm dichroic mirror, and a 535/45 emission filter. Excitation and emission filters were placed in filter wheels external to the microscope controlled by a Lambda 10-3 filter changer (Sutter Instruments) to allow for rapid acquisition of ratio images. Images were collected using Metafluor software (Universal Imaging). All images were collected on healthy cells with similar mCherry intensity, using a 40 $\times$  oil objective, and were background corrected by generating a region of interest (ROI) on a blank area of the coverslip and subtracting the fluorescence intensity of each excitation channel. The background-corrected intensities at 340 nm and 380 nm excitation were used to calculate the Fura-2 340/380 ratio.

To determine the resting  $[Ca^{2+}]$  in the cytosol, cells were treated with 5  $\mu$ M ionomycin and 5 mM EGTA in  $Ca^{2+}$ -free HBSS to obtain the ratio of the unbound indicator ( $R_{min}$ ). Cells were then washed with  $Ca^{2+}$ -free HBSS three times and treated with 5  $\mu$ M ionomycin and 10 mM  $Ca^{2+}$  in HBSS to obtain the ratio of the calcium-saturated indicator ( $R_{max}$ ).  $Ca^{2+}$  concentrations were calculated using the reported  $K_d$  value of Fura-2 and the experimentally derived  $R$ ,  $R_{min}$ ,  $R_{max}$ ,  $S_f$ , and  $S_b$  (the emission intensity at 380 nm for  $Ca^{2+}$ -free and  $Ca^{2+}$ -bound Fura-2, respectively) in each individual cell according to the following equation:  $[Ca^{2+}] = K_d \times \frac{(R - R_{min})}{(R_{max} - R)} \times \frac{S_f}{S_b}$ . Details on the microscope, sensor calibration, and conversion of Fura-2 ratios into  $Ca^{2+}$  concentrations have been described previously (1). The results were presented as the fold increase of the calcium concentration in cells transfected with pcDNA3-Flag-HBx over that in cells transfected with the empty vector.

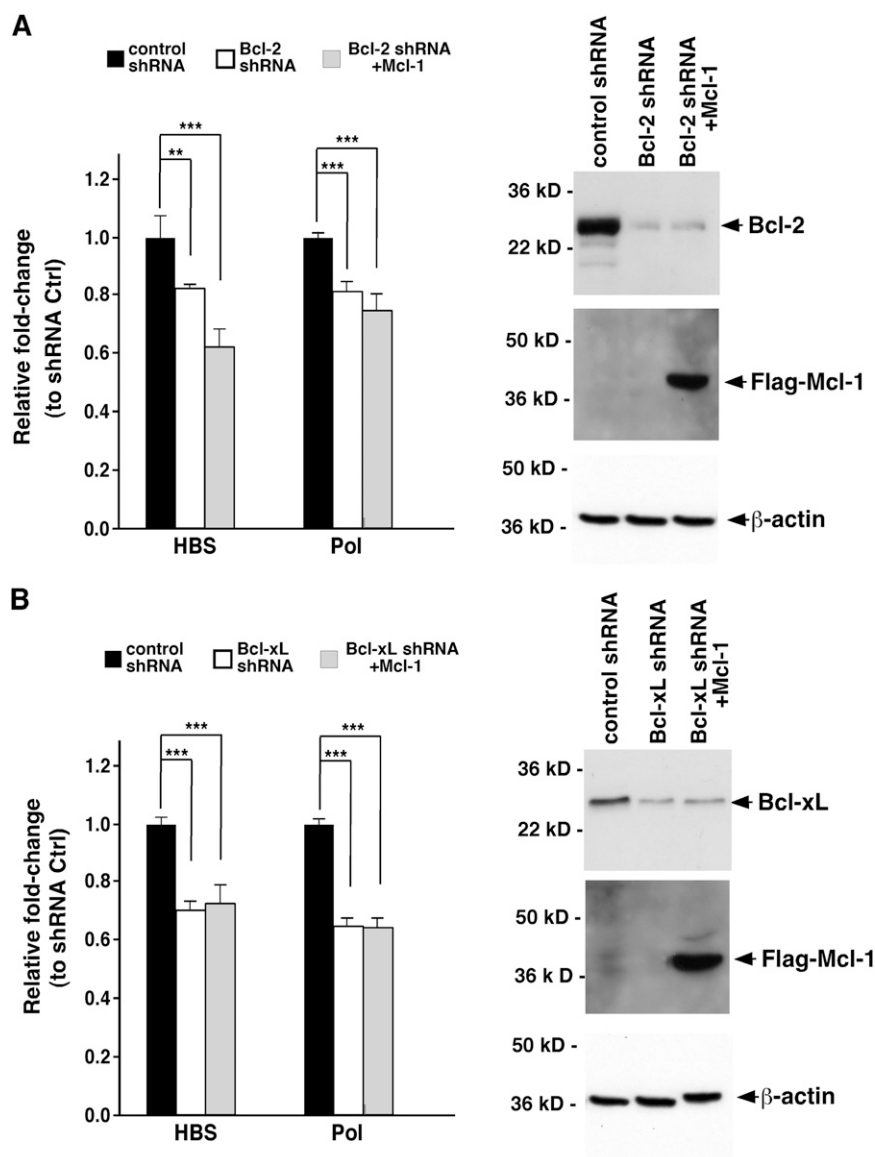
**Southern Blot Analysis.** HepG2 cells ( $3 \times 10$ -cm plate per sample) transfected with the pHBV replicon (wild type or mutant) were washed twice with cold PBS and lysed in 750  $\mu$ L NET buffer [50 mM Tris-HCl (pH 7.5), 1 mM EDTA, 100 mM NaCl, 0.5% Nonidet P-40] per 10-cm plate for 1 h. HepG2 cell lysates were clarified by centrifugation at  $12,000 \times g$  for 30 min at 4 °C. The supernatant was adjusted to 6 mM  $CaCl_2$  and treated with 100  $\mu$ g/mL of micrococcal nuclease for 30 min at 37 °C. The reaction was stopped by addition of EDTA to a final concentration of 25











**Fig. S2.** Overexpression of Mcl-1 did not prevent reduction of HBV DNA replication caused by loss of Bcl-2 or Bcl-xL. (*A and B*) (*Left*) HepG2 cells infected by lentivirus expressing control, Bcl-2, or Bcl-xL shRNA were cotransfected with 2  $\mu$ g of the pHBV replicon and 2  $\mu$ g of pcDNA3-Flag-Mcl-1 and subjected to Q-PCR analysis as described in Fig. 3D. (*Right*) shRNA knockdown efficiency and the expression level of Flag-Mcl-1 were analyzed by immunoblotting using anti-Bcl-2, anti-Bcl-xL, and anti-Flag antibodies and  $\beta$ -actin as a loading control. Data are presented as mean  $\pm$  SEM. \*\* $P < 0.01$ ; \*\*\* $P < 0.0001$ .